

## Supporting Information

### **MXene-decorated flexible Al<sub>2</sub>O<sub>3</sub>/TiO<sub>2</sub> nanofibrous mats with self-adaptive stress dispersion towards multifunctional desalination**

Yunpeng Wang,<sup>a</sup> Wanlin Xu,<sup>a</sup> Xixi Zou,<sup>a</sup> Wanlin Fu,<sup>a</sup> Xiangyu Meng,<sup>a</sup> Jingyi Jiang,

<sup>a</sup> Yiqun Zheng,<sup>b</sup> Seeram Ramakrishna,<sup>c</sup> Yueming Sun,<sup>a</sup> Yunqian Dai <sup>\*,a</sup>

<sup>a</sup> School of Chemistry and Chemical Engineering, Southeast University, Nanjing, Jiangsu, 211189, P. R. China

<sup>b</sup> School of Chemistry, Chemical Engineering, and Materials, Jining University, Qufu, Shandong, 273155, P. R. China

<sup>c</sup> NUS Centre for Nanotechnology and Sustainability (NUSCNS), National University of Singapore, 117584, Singapore

\* Address Corresponding to: daiy@seu.edu.cn

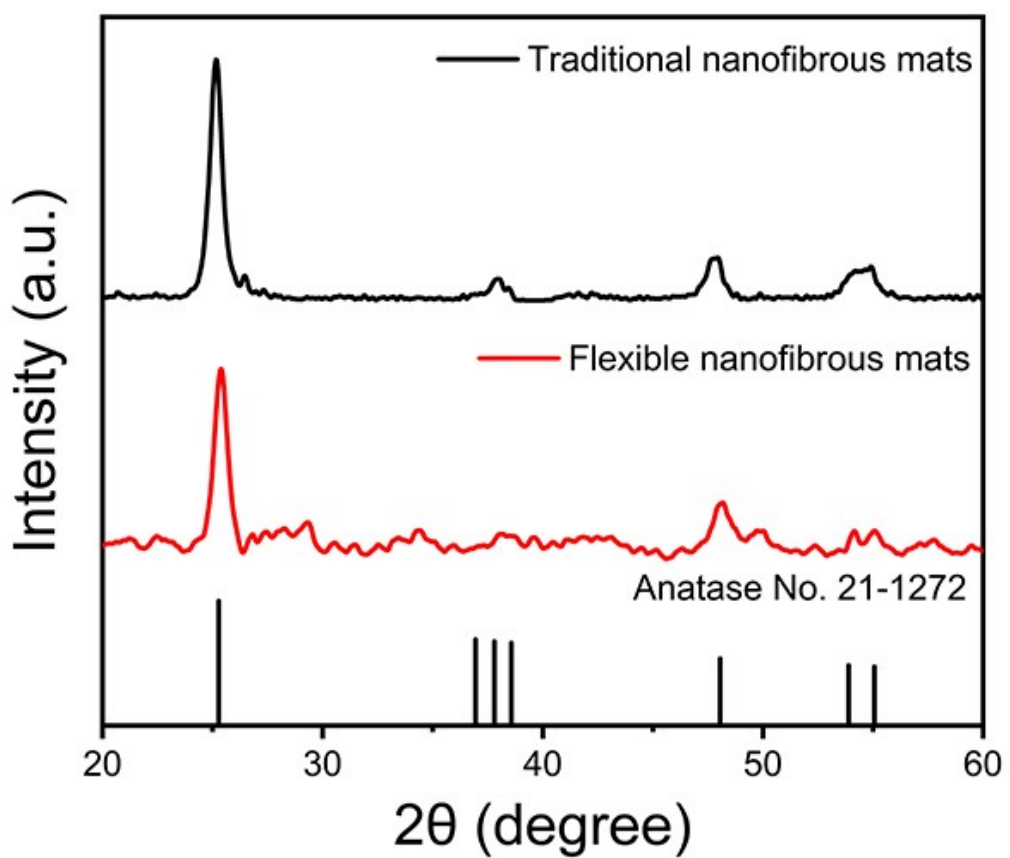


**Fig. S1.** XRD of flexible and traditional  $\text{Al}_2\text{O}_3/\text{TiO}_2$  nanofibrous mats.

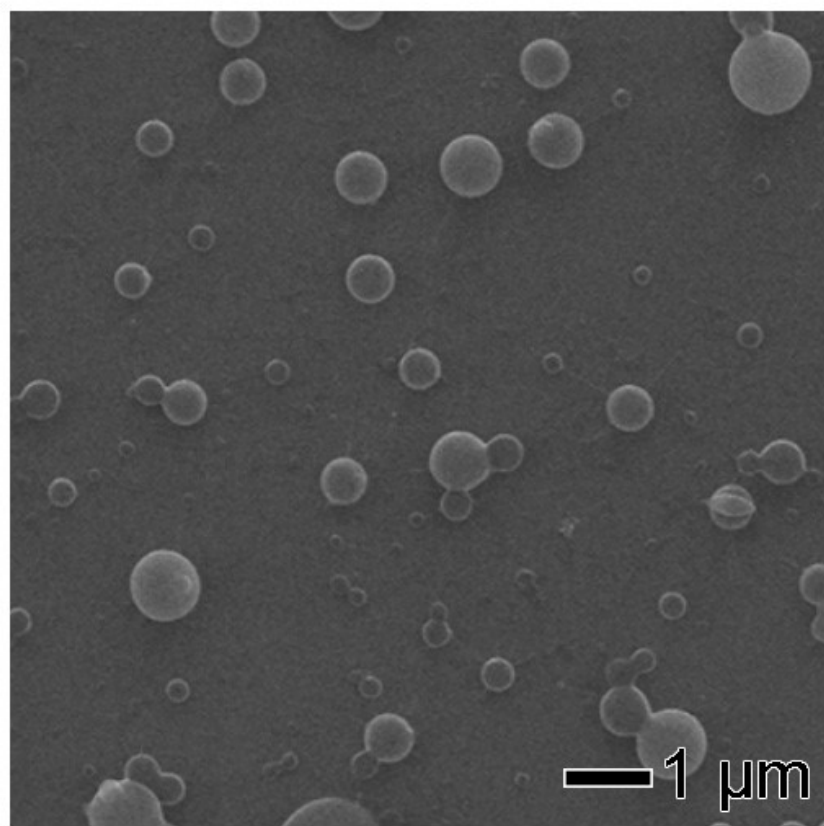


**Fig. S2.** SEM image of the  $\text{Al}_2\text{O}_3/\text{TiO}_2$  microspheres.

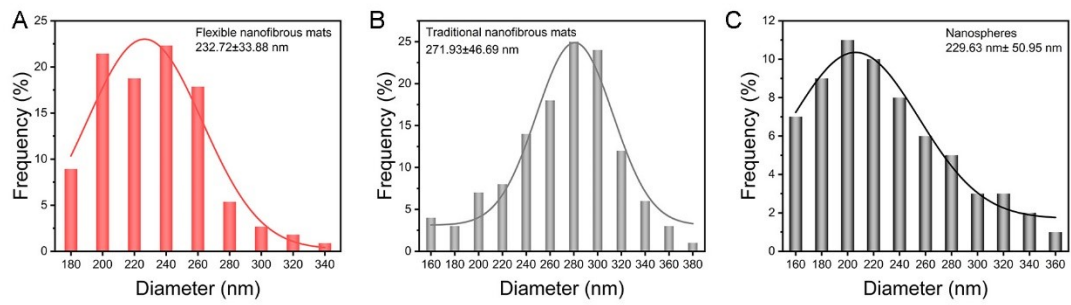


**Fig. S3.** The corresponding diameter distributions of (A) flexible, (B) traditional  $\text{Al}_2\text{O}_3/\text{TiO}_2$  nanofibrous mat and (C)  $\text{Al}_2\text{O}_3/\text{TiO}_2$  nanospheres.

The force is pushed perpendicularly within the fibrous mats.

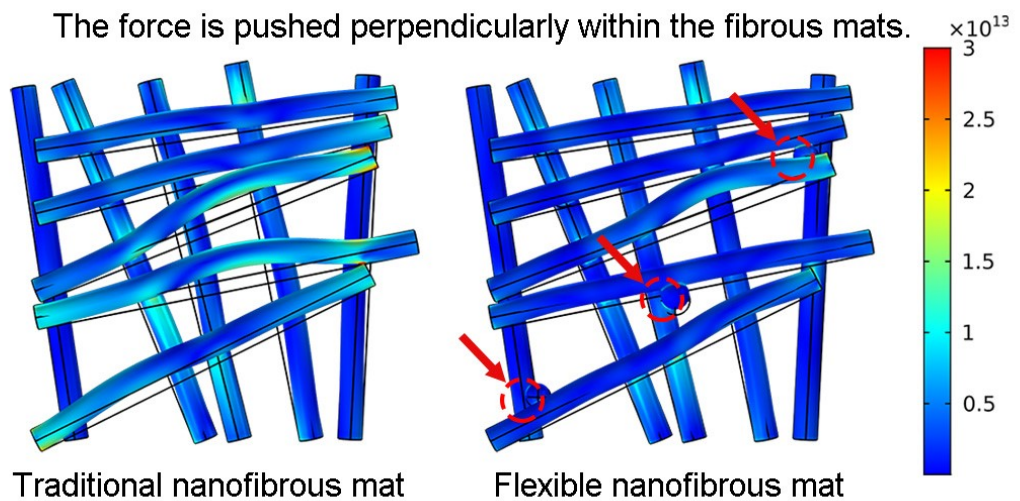


**Fig. S4.** Elastic modulus of the traditional nanofibrous mat and flexible nanofibrous mat.

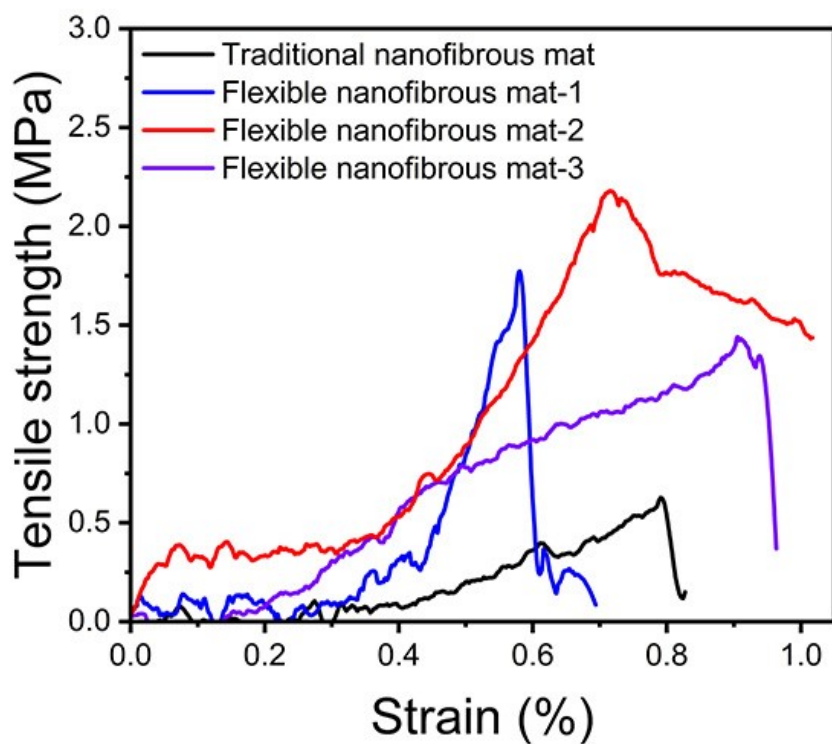


**Fig. S5.** The stress-strain curves of traditional and flexible Al<sub>2</sub>O<sub>3</sub>/TiO<sub>2</sub> nanofibrous mats.

**Table S1** Comparison of tensile strength

Materials	Tensile strength /MPa	Strain/%	Young's modulus/MPa	Reference
<b>Flexible Sn-doped SrTiO<sub>3</sub> membranes</b>	0.220	1.80	13.3	<sup>1</sup>
<b>BM-Li<sub>0.35</sub>La<sub>0.55</sub>TiO<sub>3</sub> membrane</b>	0.320	1.58	20.3	<sup>2</sup>
<b>N-CNF membrane</b>	0.880	1.69	51.8	<sup>3</sup>
<b>TiO<sub>2</sub>/carbon NFM</b>	1.14	2.20	51.8	<sup>4</sup>
<b>Co-doped-core-shell carbon NFM</b>	1.30	3.50	37.1	<sup>5</sup>
<b>SiO<sub>2</sub>-CNFs</b>	1.52	1.77	77.4	<sup>6</sup>
<b>Montmorillonite@ZrO<sub>2</sub>-SiO<sub>2</sub> membranes</b>	1.83	1.13	146	<sup>7</sup>
<b>Flexible Al<sub>2</sub>O<sub>3</sub>/TiO<sub>2</sub> nanofibrous mat-1</b>	1.77	0.581	305	This work
<b>Flexible Al<sub>2</sub>O<sub>3</sub>/TiO<sub>2</sub> nanofibrous mat-2</b>	2.18	0.715	305	This work
<b>Flexible Al<sub>2</sub>O<sub>3</sub>/TiO<sub>2</sub> nanofibrous mat-3</b>	1.44	0.905	159	This work

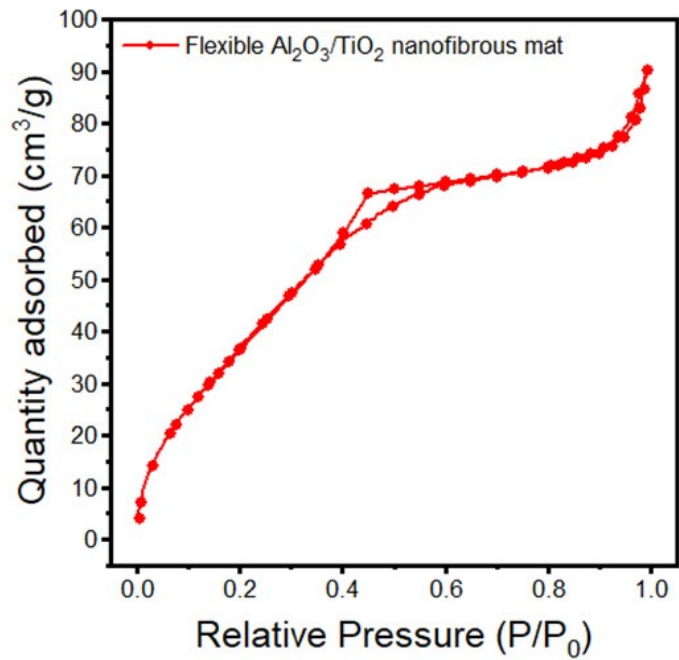


**Fig. S6.** BJH adsorption of traditional and flexible Al<sub>2</sub>O<sub>3</sub>/TiO<sub>2</sub> nanofibrous mats.

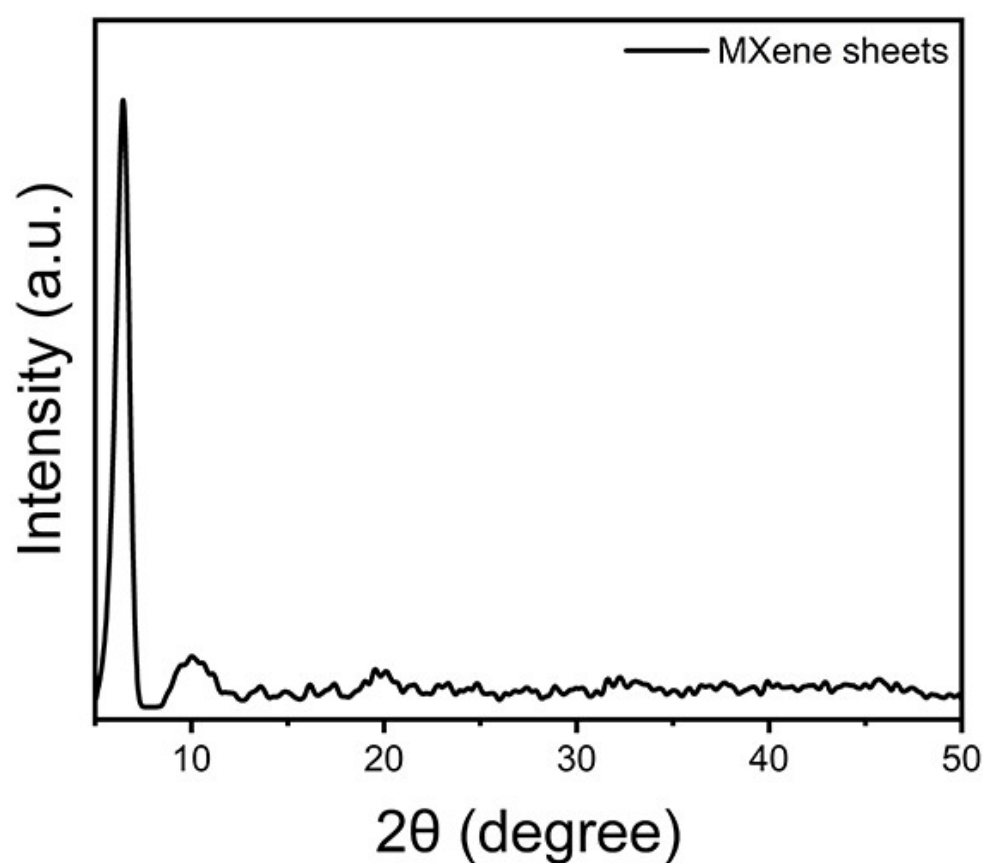


**Fig. S7.** XRD of the  $\text{Ti}_3\text{C}_2\text{T}_x$  Mxene sheets.

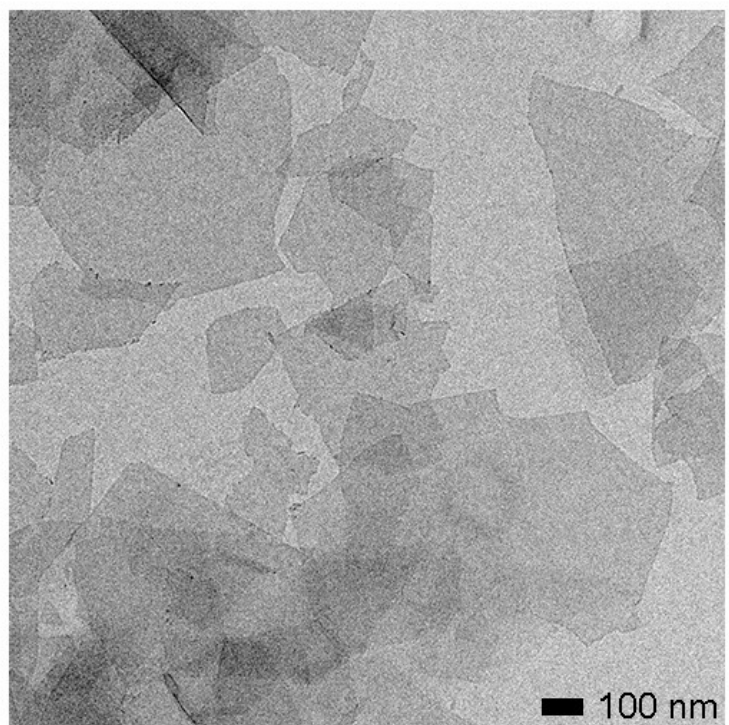


**Fig. S8.** TEM image of the Ti<sub>3</sub>C<sub>2</sub>T<sub>x</sub> Mxene sheets.

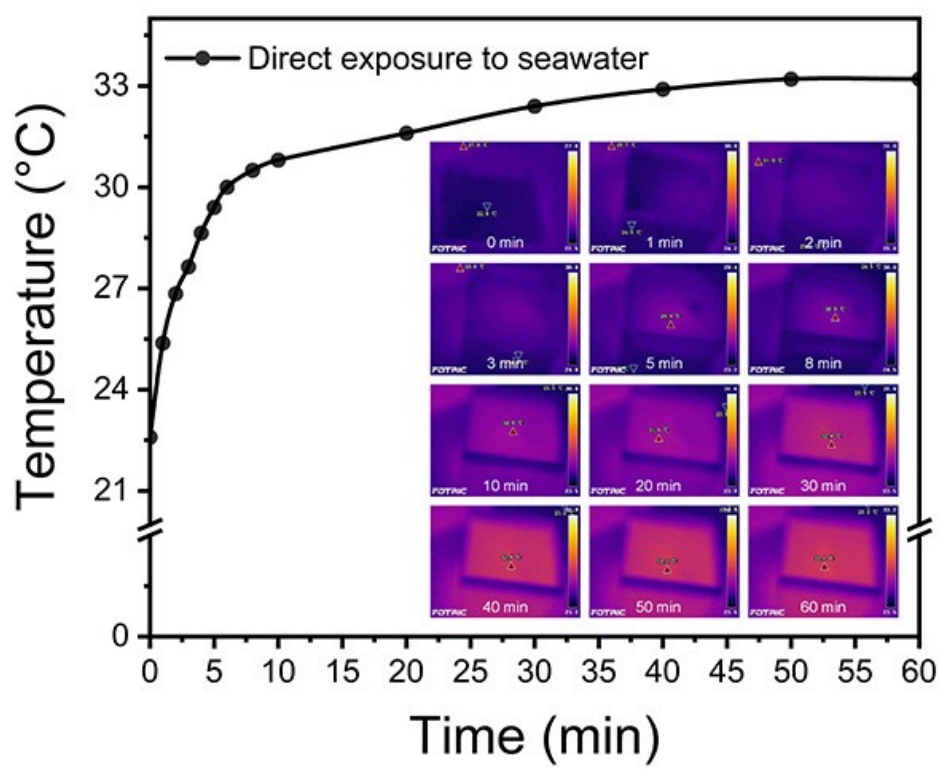


**Fig. S9.** Surface temperature change as a function of irradiation time for the water under one sun solar illumination. The inset depicts the IR thermal images showing the temperature distribution of the water.

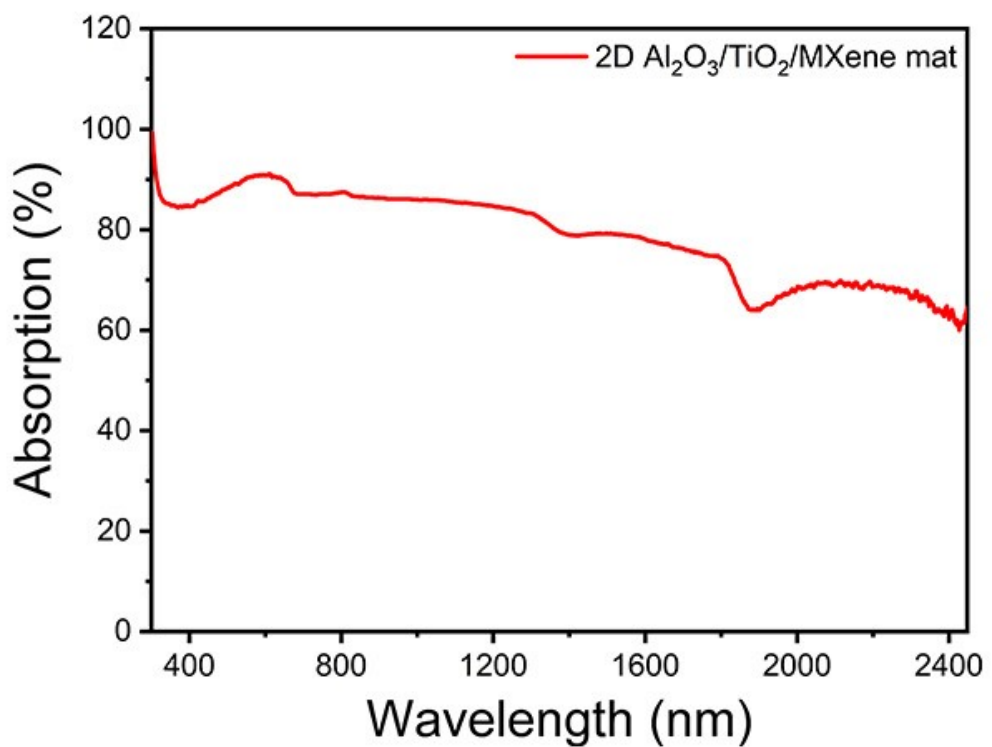


**Fig. S10.** Absorption spectra of the  $\text{Al}_2\text{O}_3/\text{TiO}_2/\text{MXene}$  mat.

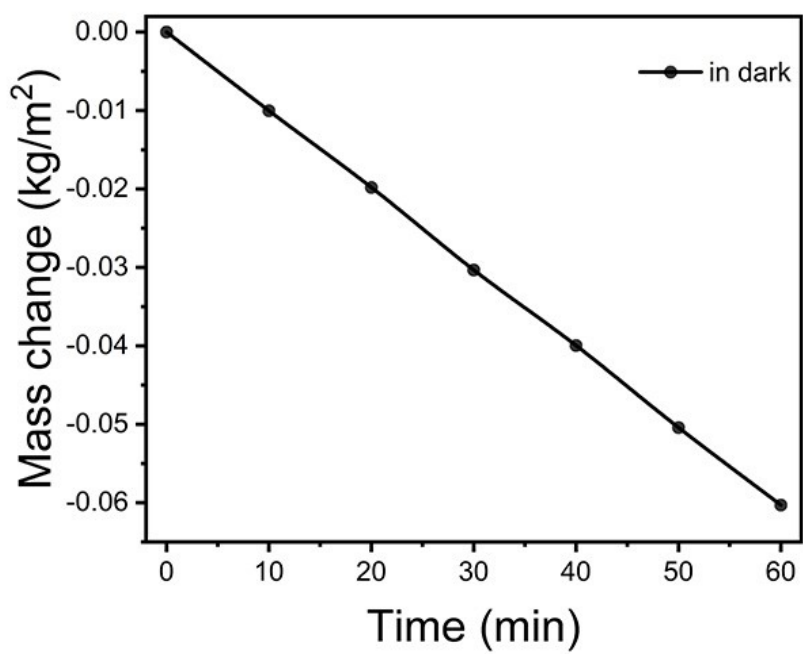


**Fig. S11.** The water mass change recording the evaporation performance of photothermal Al<sub>2</sub>O<sub>3</sub>/TiO<sub>2</sub>/Mxene mat under dark.

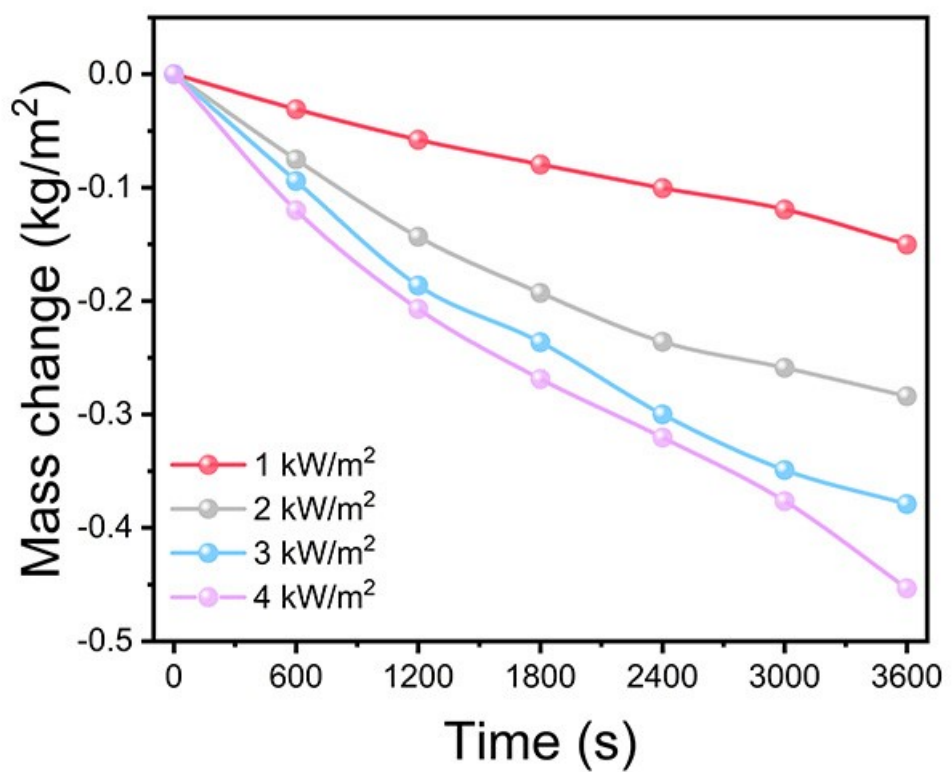


**Fig. S12.** Mass change of seawater for the flexible  $\text{Al}_2\text{O}_3/\text{TiO}_2$  mat under different solar illumination intensities.

**Table S3** Comparison of conversion rates in Figure. 3

Materials	evaporation rate (kg·m <sup>-2</sup> ·h <sup>-1</sup> )	light-to-vapor energy conversion efficiency (%)	Reference
A cobalt nanoparticle-carbonaceous nanosheets/MXene foam	1.39	93.4	8
Flexible and superhydrophobic MXene based fabric composites	1.26	93.3	9
Nanocomposite MXene@rGO membrane	1.33	85.2	10
PVDF/graphene membrane	1.20	84.0	11
Graphite-wood	1.15	80.0	12
A metal-Si hybrid nanowire	1.12	72.8	13
Carbon black nanoparticles of Janus absorbers	1.30	72.0	14
Photothermal Al <sub>2</sub> O <sub>3</sub> /TiO <sub>2</sub> /Mxene mat	1.43	102	this work

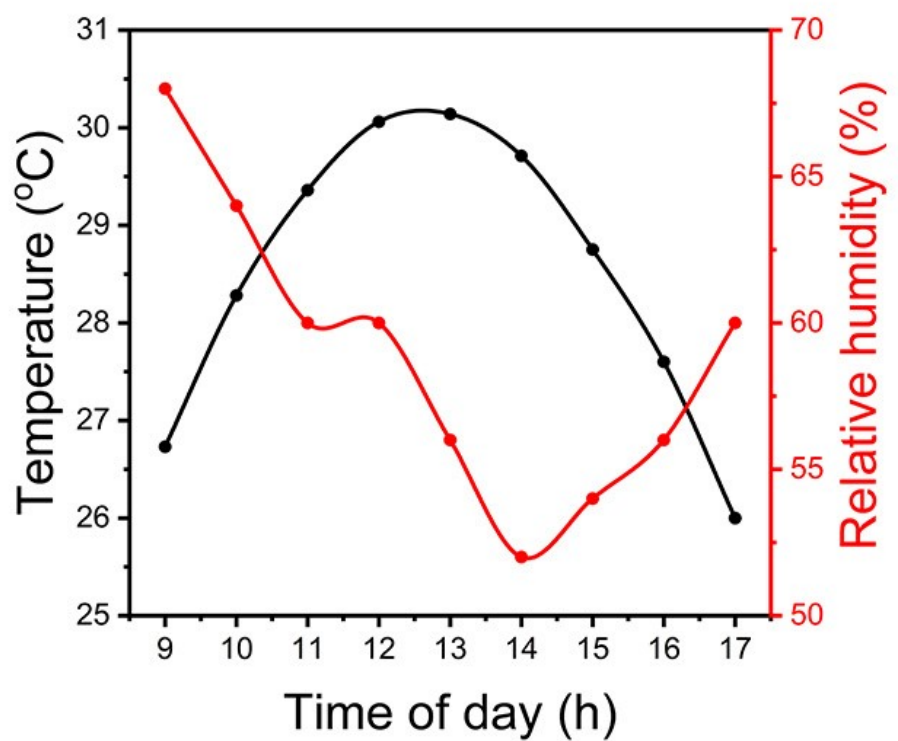


**Fig. S13.** Air temperature and relative humidity were recorded from 9:00 to 17:00.

**Table S3** Comparison of density of the 3D photothermal evaporator to previous reports

in Figure. 5

Materials	Density (mg/cm <sup>3</sup> )	Reference
Elastic 3D fibrous aerogels	7.02	<sup>15</sup>
Porous 3D nanofibrous Kevlar aeroge	11.9	<sup>16</sup>
Ultralight BNNTs/rGO aerogel	16.3	<sup>17</sup>
Self-assembled 3D networks of aramid nanofiber composites	20.0	<sup>18</sup>
Aramid nanofiber aerogel	25.0	<sup>19</sup>
ANF-derived carbon aerogel	51.7	<sup>20</sup>
Polyimide/MXene aerogel	69.7	<sup>21</sup>
Resultant graphene-polydopamine-bovine serum albumin aerogel	88.0	<sup>22</sup>
3D Al <sub>2</sub> O <sub>3</sub> /TiO <sub>2</sub> /Mxene evaporator	6.41	This work

## References

- 1 X. Gao, F. Zhou, M. Li, X. Wang, S. Chen and J. Yu, *ACS Appl. Mater. Interfaces*, 2021, **13**, 52811-52821.
- 2 X. Li, Y. Zhang, L. Zhang, S. Xia, Y. Zhao, J. Yan, J. Yu and B. Ding, *Small*, 2022, **18**, 2106500.
- 3 J. Wang, Z. Wang, J. Ni and L. Li, *Energy Storage Mater.*, 2022, **45**, 704-719.
- 4 P. Zhang, S. Zhang, D. Wan, P. Zhang, Z. Zhang and G. Shao, *J. Hazard. Mater.*, 2020, **395**, 122639.
- 5 Z. Xu, J. Zhu, J. Shao, Y. Xia, J. Tseng, C. Jiao, G. Ren, P. Liu, G. Li, R. Chen, S. Chen, F. Huang and H. Wang, *Energy Storage Mater.*, 2022, **47**, 365-375.
- 6 Z. Zhu, L. Zhong, Z. Zhang, H. Li, W. Shi, F. Cui and W. Wang, *J. Mater. Chem. A*, 2017, **5**, 25266-25275.
- 7 X. Mao, J. Hong, Y. Wu, Q. Zhang, J. Liu, L. Zhao, H. Li, Y. Wang and K. Zhang, *Nano Lett.*, 2021, **21**, 9419-9425.
- 8 X. Fan, Y. Yang, X. Shi, Y. Liu, H. Li, J. Liang and Y. Chen, *Adv. Funct. Mater.*, 2020, **30**, 2007110.
- 9 W. Xiao, J. Yan, S. Gao, X. Huang, J. Luo, L. Wang, S. Zhang, Z. Wu, X. Lai and J. Gao, *Desalination*, 2022, **524**, 1155475.
- 10 P. Ying, B. Ai, W. Hu, Y. Geng, L. Li, K. Sun, S. Tan, W. Zhang and M. Li, *Nano Energy*, 2021, **89**, 106443.
- 11 C. Huang, J. Huang, Y. Chiao, C. Chang, W. Hung, S. Lue, C. Wang, C. Hu, K. Lee, H. Pan and J. Lai, *Adv. Funct. Mater.*, 2021, **31**, 2010422.
- 12 T. Li, H. Liu, X. Zhao, G. Chen, J. Dai, G. Pastel, C. Jia, C. Chen, E. Hitz, D. Siddhartha, R. Yang and L. Hu, *Adv. Funct. Mater.*, 2018, **28**, 1707134.
- 13 B. Joo, I. Kim, I. Han, H. Ko, J. Kang and G. Kang, *Appl. Surf. Sci.*, 2022, **583**, 152563.
- 14 W. Xu, X. Hu, S. Zhuang, Y. Wang, X. Li, L. Zhou, S. Zhu and J. Zhu, *Adv. Energy Mater.*, 2018, **8**, 1702884.
- 15 X. Meng, X. Peng, Y. Wei, S. Ramakrishna, Y. Sun and Y. Dai, *Chem. Eng. J.*, 2022, **437**, 135444.

- 16 Q. Cheng, Y. Liu, J. Lyu, Q. Lu, X. Zhang and W. Song, *J. Mater. Chem. A*, 2020, **8**, 14243-14253.
- 17 M. Wang, T. Zhang, D. Mao, Y. Yao, X. Zeng, L. Ren, Q. Cai, S. Mateti, L. Li, X. Zeng, G. Du, R. Sun, Y. Chen, J. Xu and C. Wong, *ACS Nano*, 2019, **13**, 7402-7409.
- 18 H. He, X. Wei, B. Yang, H. Liu, M. Sun, Y. Li, A. Yan, C. Tang, Y. Lin and L. Xu, *Nat. Commun.*, 2022, **13**, 4242.
- 19 C. Xie, L. He, Y. Shi, Z. Guo, T. Qiu and X. Tuo, *ACS Nano*, 2019, **13**, 7811-7824.
- 20 B. Zhou, G. Han, Z. Zhang, Z. Li, Y. Feng, J. Ma, C. Liu and C. Shen, *Carbon*, 2021, **184**, 562-570.
- 21 Y. Yang, W. Fan, S. Yuan, J. Tian, G. Chao and T. Liu, *J. Mater. Chem. A*, 2021, **9**, 23968-23976.
- 22 A. Masud, C. Zhou and N. Aich, *Environ. Sci.- Nano*, 2021, **8**, 399-414.